Polar-horizontal versus polar-vertical reverse-tilt-domain walls: Influence of a pretilt angle below the nematic-isotropic phase transition

Ji-Hoon Lee, Timothy J. Atherton, Daeseung Kang,* Rolfe G. Petschek, and Charles Rosenblatt
Department of Physics, Case Western Reserve University, Cleveland, Ohio 44106-7079, USA
(Received 30 April 2008; published 15 August 2008)

On cooling through the isotropic-to-nematic phase transition in a cell whose substrates induce a large pretilt angle θ_0 from the vertical direction, but with no preferential azimuthal orientation, tilt domains appear. The boundary walls between reverse tilt domains are found to be bendlike and twistlike when $\theta_0(T=T_{NI})$ is sufficiently large just below the isotropic-nematic phase transition temperature T_{NI}—i.e., for a nearly planar orientation. Here the director becomes planar approximately midway through the wall, and we refer to this type of wall as "polar horizontal," which is topologically stable. However, if $\theta_0(T=T_{NI})$ is sufficiently small just below T_{NI}—i.e., closer to vertical orientation—a splay like and twistlike domain wall obtains, where the director is vertically oriented approximately midway through the wall; we refer to this type of wall as "polar vertical," whose stability depends on the anchoring. On cooling through the nematic phase, the pretilt angle θ_0 decreases, with the director aligning closer to the vertical orientation. Nevertheless, the structures of both types of domain walls remain unchanged on variation of θ_0 with temperature owing to topological constraints and also are unchanged after the application and removal of a large electric field. We examine the structure of domain walls for the liquid crystal ZLI-4330 (Merck) as a function of pretilt angle $\theta_0(T=T_{NI})$ and calculate a critical value $\theta_0^c(T=T_{NI})$ of the pretilt angle just below T_{NI} for which the predominance of domain walls crosses over from polar horizontal to polar vertical.

DOI: 10.1103/PhysRevE.78.021708 PACS number(s): 61.30.Jf

A reverse-tilt-domain (RTD) wall in liquid crystals corresponds to the boundary between two regions across which the director $\hat{n}$ varies azimuthally by a large angle, often as large as π. Most commonly this occurs in a planar cell when the liquid crystal is subjected to an applied electric or magnetic field above the Freedericksz transition threshold: In one region the director has a polar orientation θ and an azimuthal orientation φ with respect to the wall that separates the two regions and in an adjacent region an orientation $\theta, \varphi+\pi$ [1,2]. Such a RTD structure may be found in planar cells treated for uniform azimuthal orientation and tends to diminish the optical quality—including contrast, symmetry, and response time—of devices based on this geometry. Thus, understanding and controlling these structures have been important concerns. Early on it was discovered that RTDs and their associated walls can be obviated by introducing a small uniform pretilt angle relative to the planar orientation, although with a slight diminution in the symmetry of the device's optical properties. But until recently there has been little understanding of the nature of the domain walls and their energetics. In a previous paper we reported on the structure of textures due to RTDs that occur naturally in cells treated for high polar pretilt angle θ_0, but with no preferred azimuthal orientation [3], where we define θ_0 as the angle relative to the *vertical* direction; thus, $\theta_0=0$ would correspond to homeotropic (i.e., vertical) orientation. Recently we found that the structure of the RTDs and their associated walls is extremely sensitive to baking conditions of the polyimide and that there actually exist two topologically distinct types of walls with markedly different optical appearances. The existence of one type of wall or the other depends strongly on the pretilt conditions just below the nematic-isotropic phase transition temperature. In this paper we explore these issues, characterizing the very different natures of the walls, their energetics, and the influence of θ_0, which varies with temperature within the nematic phase. In particular, we show that when θ_0 is large (i.e., the director is close to planar) just below the nematic-isotropic transition temperature T_{NI}, the RTD wall is of the "polar-horizontal" type, wherein the director is planar approximately midway through the domain wall. When $\theta_0(T=T_{NI})$ is smaller—i.e., closer to the vertical orientation—RTD walls of the "polar-vertical" type appear simultaneously with those of the polar-horizontal type, wherein the director is vertical approximately midway through the domain wall. Additionally, we find that polar-vertical walls are associated intimately with topological defects known as partial disclinations. A calculation for the energetics of the two types of domain walls is presented and compared with observations. The results shed light on RTDs and present the possibility of tailoring the substrates either to eliminate the RTDs entirely or to produce an array of controlled RTDs and walls.

Several pairs of indium-tin-oxide-coated glass slides were cleaned and spin coated with the polyamic acid SE1211 (Nissan Chemical Industries), then baked for a time t_b at a temperature of 230 °C. The baking time t_b spanned the range from 0.75 h to 3 h, with longer baking times associated with larger pretilt angles θ_0 at T_{NI}. After baking, the imidized SE1211 has a relatively rigid backbone that promotes planar alignment, as well as alkyl side chains that promote homeotropic alignment [4–6]. Had we baked using the manufacturer's specifications of 180 °C for 50 min, SE1211 would have induced homeotropic (vertical) alignment in the liquid crystal. Higher temperature and longer baking, however, further

*Permanent address: Department of Electrical Engineering, Soongsil University, Seoul, Republic of Korea.

imidize the backbone and cleave off a fraction of the side chains, resulting in a large, controllable, and robust pretilt angle θ_0 relative to the vertical direction; this is the case for the baking regimen used in our experiments. Without being rubbed, each pair of substrates was placed together, separated by glass spacer beads dispersed in a UV curable epoxy, and cemented by exposure to ultraviolet light. The thicknesses of the empty cells were measured by interferometry and found to be $d \approx 10$ μm, with a cell-to-cell distribution of approximately ± 0.5 μm around this value. Each cell was filled with liquid crystal mixture ZLI-4330 (Merck) in the isotropic phase and then cooled through the clearing temperature $T_{NI}=82$ °C to room temperature in the nematic phase. All cells displayed naturally occurring RTDs and RTD walls, which will be discussed below.

In order to determine pretilt angle θ_0 versus temperature T and baking time t_b, a second set of cells was prepared, again using indium-tin-oxide-coated glass slides and spin coated with SE1211. Before cementing, however, both surfaces were rubbed very gently with a cotton cloth (Yoshikawa Chemical Co., YA-25-C, average fiber density was $\sigma_f = 1040$ threads cm^{-2}) using an Optron rubbing machine, which has a roller radius of $r=4$ cm. The fiber pile was deformed by approximately $\delta=0.001$ cm. The slide was translated once ($N=1$) with velocity $V=0.28$ cm s^{-1} beneath the rubbing cylinder, with the roller rotating at a rate $\nu=10$ rotations per second. The "rubbing strength" n_f is defined as the number of fibers passing a position of unit width [7] and is given by $n_f \approx (2r\delta)^{1/2} 2\pi N \nu r \sigma_f / V$, which for our case is $n_f = 8.2 \times 10^4$ cm^{-1}. This rubbing regimen is considerably weaker—by one to two orders of magnitude—than that used in experiments for which the pretilt angle was controlled by the rubbing strength [8]. Thus, it is expected that our weak rubbing would have no significant effect on the polar pretilt angle. Each pair of slides was placed together, separated by glass bead spacers dispersed in a UV curable epoxy, in an antiparallel configuration, and the thickness was measured by interferometry. Typical thicknesses d again were $d \sim 10$ μm and were measured with an uncertainty of ± 0.2 μm. The cells then were filled with liquid crystal ZLI-4330. Light from a He-Ne laser (wavelength $\lambda = 633$ nm) passed consecutively through a polarizer, a Babinet-Soleil compensator, the cell, and an analyzer and into a detector. A potential difference of 50 V at frequency 1000 Hz was placed across the cell, driving the director of the negative dielectric anisotropy liquid crystal to be parallel to the substrates, except *very* close to the substrates. The compensator was adjusted to cancel the retardation $\alpha [= 2\pi d \Delta n / \lambda]$ of the cell, where Δn is the birefringence. (Values for the ordinary and extraordinary refractive indices n_o and n_e, respectively, as well as the birefringence $\Delta n = n_e - n_o$, were obtained using an Abbe refractometer.) This configuration corresponds to the maximum optical retardation, which is associated with a planar cell. We then slowly reduced the voltage to zero, *continuously* adjusting the compensator so that it canceled the cell's retardation. In this way we are able to determine the retardation difference between a fully planar director at high voltage and the pretilted director at zero voltage, without the ambiguity associated with integer multiples of 2π in the retardation. Since the retardation at high voltage is equal to $2\pi d \Delta n / \lambda$ and the retardation at zero voltage has the same form, except that one needs to use the effective birefringence $\Delta n_{eff}(\theta_0) = [\cos^2 \theta_0 / n_o^2 + \sin^2 \theta_0 / n_e^2]^{-1/2}$, which depends on θ_0, we were able to extract θ_0. This procedure was repeated to extract θ_0 vs T for each cell and thus for each baking time t_b; data for θ_0 are shown in Fig. 1. It is apparent that θ_0 increases with increasing temperature, reaching a maximum at T_{NI}. It is the value at the transition—viz., $\theta_0(T=T_{NI})$—that determines the properties of the RTDs and domain walls as the liquid crystal is cooled from the isotropic into the nematic phase. As an aside, we note that the pretilt angle is smaller (director is less planar) in the present work than in Ref. [3] owing to the lower baking temperature used herein. The lower baking temperature has the effect of maintaining the side chains and reducing imidization of the backbone, thus promoting vertical alignment [4].

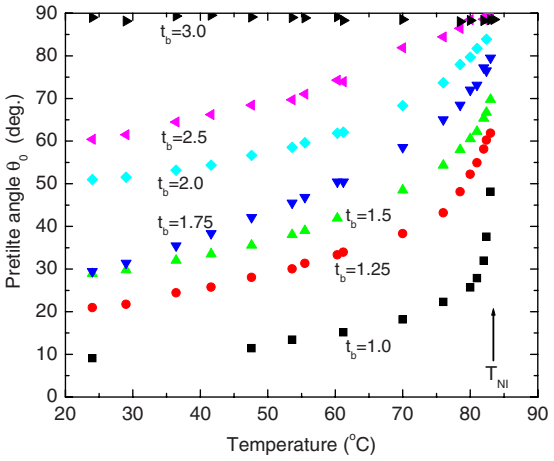

FIG. 1. (Color online) Pretilt angle θ_0 vs temperature T for a series of different baking times t_b.

Figure 2 shows a photomicrograph of the unrubbed cell, whose substrates had been baked for $t_b=2.5$ h, at room temperature. Qualitatively the appearance of the cell is very similar to that of the cell baked for 3 h: There is a background schlieren texture that represents a slow azimuthal variation of the projection of the director in the plane of the cell, with topological defects of strength $|s|=1$. This is consistent with the requirement that such topological defects or disclinations in the tilted alignment are required to have a 2π

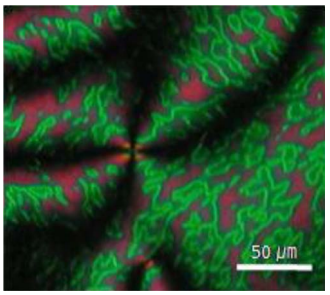

FIG. 2. (Color online) Photomicrograph of unrubbed cell and liquid crystal whose polyimide-coated glass substrates were baked for 2.5 h at 230 °C. Polar-horizontal RTD walls and background schlieren texture are easily visible.

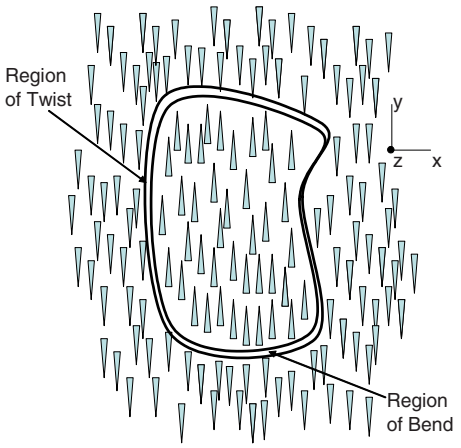

FIG. 3. (Color online) Schematic diagram of director alignment in the domains around the polar-horizontal RTD wall. The schematic of the wall represents the tendency of the wall to be darkest at the edges, where θ_0 is smallest, and brightest in the center, where $\theta_0=90°$. The vertex of isosceles triangle represents the z component of director pointing downward, and the base of the triangle represents the z component pointing upward. Where the projection of the director in the xy plane is parallel to the wall, the director undergoes a twist deformation across the domain wall; where the projection of the director is perpendicular to the filament, the director undergoes a primarily bend like deformation across the domain wall.

rotation of this alignment. That the schlieren brushes rotate between crossed polarizers as the cell is rotated indicates that the azimuthal orientations at the top and bottom surfaces are (nearly) the same. But since the two surfaces are untreated and would promote random azimuthal order, this behavior suggests that the preference for a surface-specific azimuthal orientation on *first* cooling below T_{NI} is weak; i.e., the azimuthal anchoring strength coefficient initially is very small [9]. Weak azimuthal anchoring would facilitate a uniform orientation through the cell thickness, as observed experimentally. But as will be discussed below, the anchoring strength does not remain weak, but rather increases with time as the liquid crystal molecules adsorb onto the surface and a surface memory effect develops [10].

Additionally, we find in Fig. 2 a large concentration of polar horizontal walls that separate reverse tilt domains. Because of the very high pretilt angle at T_{NI}, a domain wall in which the director passes from $+\theta_0$ through $\theta=\pi$ (horizontal) to $-\theta_0$ is energetically inexpensive. Figure 3 is a schematic representation of the director orientation in the two domains. When the projection of the director is perpendicular to the domain wall, the deformation through the wall is primarily bend, with a small component of splay; when the projection of the director is parallel to the domain wall, the deformation through the wall is primarily twist. As the temperature is lowered from T_{NI} and θ_0 decreases, the intensity contrast in Fig. 2 between the domain wall and the RTDs on either side increases, where the optical retardation is maximum in the center of the wall (where the director remains horizontal), but decreases on either side. As noted previously [3], if the cell is heated into the isotropic phase and cooled back into the nematic phase, the polar-horizontal walls reappear in the same places, another indication of a strong surface memory effect [10].

For shorter baking times ($t_b \leqslant 2$ h) the pretilt angle θ_0 at $T=T_{NI}$ is reduced, resulting in several changes. First, on cooling into the nematic phase we find that the spatial density of domain walls is smaller than for cells prepared with longer baking times. This trend continues monotonically with decreasing t_b, so that for cells baked for $t_b=0.75$ h, the density of domain walls is quite small. We believe that this trend is due to the weaker azimuthal coupling between polyimide and liquid crystal for short baking times—indeed, the weaker coupling is manifested in the corresponding smaller polar pretilt angle. In consequence, the local azimuthal anchoring is weaker for smaller t_b, and thus on nucleation of the nematic phase spatially homogeneous domains tend to be larger, with a resulting decrease in the spatial density of domain walls. A related observation, which will be treated in more detail elsewhere, is that the surface memory effect is weaker for cells baked for shorter times. On heating these cells back into the isotropic phase and then cooling again into the nematic phase, we found that the domain wall structure no longer is identical to the initial structure observed on the first cooling into the nematic: Some domain walls reappear in the same locations, but other domain walls do not reappear and new domain walls are observed. This trend of a less robust surface memory effect with decreasing t_b becomes particularly noticeable for our shortest baking times, where there is no apparent memory effect at all. These two observations—viz., a decrease in domain wall density and a decreased memory effect for smaller t_b—both suggest weaker azimuthal interactions with decreasing $\theta_0(T=T_{NI})$. A third qualitative difference is that the polar-horizontal walls, when the cell is viewed at room temperature, exhibit internal structure and tend to be brighter relative to the background than for cells baked at longer times. The reason is straightforward and can be understood from the $\theta_0(T)$ data in Fig. 1. Because θ_0 decreases with decreasing temperature, cells baked for shorter times have a significantly smaller pretilt angle—i.e., the director is closer to the vertical orientation—at room temperature. On traversing the polar-horizontal domain wall from one domain to the adjacent RTD, the optical retardation for walls in cells baked for shorter times undergoes a large variation from a minimum at one edge of the wall to a maximum in the center and to a minimum at the other wall edge. For sufficiently small t_b—i.e., when the director alignment is close to vertical in the absence of defects—the optical retardation α even can vary by more than 2π, and thus one may find one (or more) black stripes parallel to the bright stripe in the center of the wall.

Perhaps the most significant difference between the cells baked for longer times and those baked for $t_b \leqslant 2$ h is the appearance of topologically distinct polar-vertical domain walls. These walls appear as a single dark stripe, because for sufficiently small $\theta_0(T=T_{NI})$ the director's polar angle θ rotates through the vertical ($\theta=0$) direction midway through the wall. From one point of view, the appearance of these domain walls with decreasing tilt is physically quite reasonable. As the alignment of the liquid crystal becomes closer and closer to vertical, it takes decreasing amounts of energy to change from one tilt domain to another by going through the vertical rather than through the horizontal orientation.

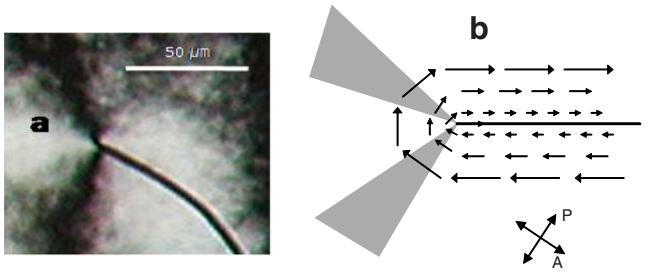

FIG. 4. (Color online) Polar-vertical domain wall terminating in a two brush point defect. (b) Schematic representation of one possible director pattern, where the length of the arrows represents the magnitude of the projection of the director in the plane. The director is oriented vertically at the domain wall. **P** and **A** correspond to polarizer and analyzer.

The polar horizontal domain walls are topologically stable, so that once they form, they cannot be eliminated via an azimuthal reorientation of the alignment at the surfaces. On the other hand, the vertical domain walls are *not* topologically stable in this sense—it is only the preferred alignment on either side of the defect that has been rotated by an angle close to π that stabilizes these defects. This strongly suggests that, even for these relatively low pretilt samples—i.e., close to vertical alignment—there is a rather stronger anchoring for the orientation of the projection of the tilted nematic director than for its sign. It also would seem to suggest that this orientation is relatively quickly "remembered" by the surface [10], so that it can prevent the thermodynamically favored dissolution of this wall into a slow azimuthal reorientation. In all cases for $0.75 \leqslant t_b \leqslant 2$ h, the polar-vertical and polar-horizontal walls appear in the same cell simultaneously. Although both types of walls can appear as closed loops, separating an islandlike RTD from the surrounding region, the polar-vertical walls also tend to be related intimately to topological defects associated with the background schlieren texture. Figure 4(a) shows a vertical domain wall, along with two brushes, terminating at a topological defect. Figure 4(b) is a schematic representation of the likely director pattern, where the length of the arrow is indicative of the projection of the director into the plane of the cell. Although the director pattern shows some similarities to a typical $s = \frac{1}{2}$ defect, here the director rotates out of the cell plane and becomes vertical along the polar-vertical wall. As this rotation is half that which is required by topology and the remaining rotation takes place through the wall, we call this a "partial disclination." When the cell is rotated under crossed polarizers, the brushes remain approximately in the same place. These dark brushes correspond to where the orientation of the projection of the midcell nematic director is parallel and perpendicular to the polarizers. As this projection rotates by π, moving around the center of this defect, the brushes remain at approximately the same angle relative to the defect as the cell is rotated. However, the dark polar-vertical wall remains dark and rotates with the cell, as the director passes through the vertical direction inside the wall. We note that a similar defect is, in principle, possible for a polar-horizontal wall: This is essentially the colocation of the partial disclination described above and the boundary between a polar-vertical and polar-horizontal walls, as will be discussed below. Unlike this partial disclination, it requires an ordinary nematic disclination and topological singularity in the director to pass from one surface of the cell to the other. However, we have never observed such a defect.

A second example is shown in Fig. 5(a), where the polar-vertical wall does not terminate, but rather passes through the junction of two brushes at a topological defect. It turns out that the appearance of only two brushes (as opposed to four brushes) is an accident of the polarizer and analyzer orientations, which are parallel and perpendicular to the polar-vertical wall as it passes through the defect. Figure 5(b) is a schematic representation of the director orientation for this defect pattern. Here the projection of the director can be either radial or circumferential. Consider the case of a radial defect: As the director passes through the polar-vertical wall, its projection in the cell plane changes by an azimuthal angle of approximately, but less than, π. *If* this angle instead were equal to π, we would expect to observe schlieren-like brushes along the polar-vertical wall direction, thereby partially obscuring the polar-vertical wall. But because these brushes are not observed, we believe that the two domains

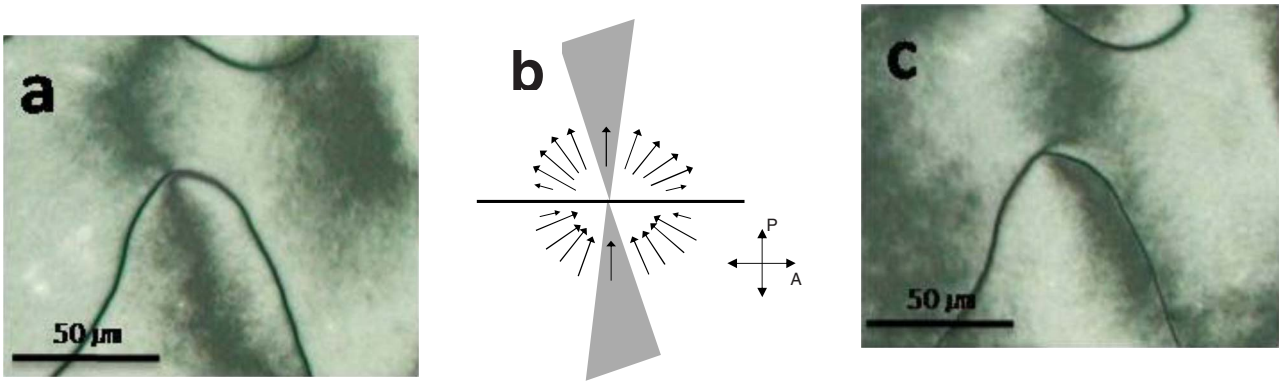

FIG. 5. (Color online) Polar-vertical domain wall passing through a point defect. (b) Schematic representation of one possible director pattern, where the length of the arrows represents the magnitude of the projection of the director in the plane. **P** and **A** correspond to polarizer and analyzer. Notice that for this case (i) there is an azimuthal discontinuity $\Delta\varphi < \pi$ across the RTD wall and (ii) the director is oriented vertically at the RTD wall. (c) Here the cell is rotated by an angle 35° between crossed polarizers. Notice the large difference in brightness on either side of the RTD wall, confirming the azimuthal discontinuity $\Delta\varphi$ across the wall.

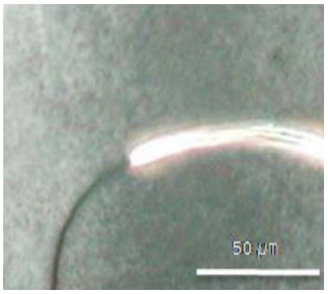

FIG. 6. (Color online) Image of polar horizontal RTD wall abutting a polar-vertical RTD wall.

separated by the polar-vertical wall differ by an azimuthal angle $\Delta\varphi < \pi$, thus facilitating a sharp dark wall (where the director is oriented vertically) in a brighter background without the usual schlieren-like brushes. This model is borne out by Fig. 5(c), in which the cell is rotated between crossed polarizers by an angle 35°. Notice that one side of the wall is dark, whereas the other side of the wall is bright. If the azimuthal discontinuity $\Delta\varphi$ across the polar-vertical wall were sufficiently close to π, a pair of schlieren-like brushes would have overlapped the wall. This is not the case. Here, when the cell is rotated between crossed polarizers, the two brushes remain fixed with respect to the polarizer and analyzer, but the polar-vertical wall rotates with the cell.

A third example of a polar-vertical wall is shown in Fig. 6. Here the polar-vertical wall terminates, abutting the end of a polar-horizontal wall. Topologically, this can occur for twistlike, bendlike, or some combination of elastic distortions through the two walls, although it is necessary that there be a disclination along the plane at which the two types of walls meet. This arrangement suggests that each of the two types of walls nucleates at different points along the boundary between the two RTDs and propagates to their meeting point. That one type of wall does not dominate and force the other type of wall to retreat is a result of the topological defect at the boundary between the walls: One type of wall cannot change continuously into the other type.

In Ref. [3] we examined the energetics of a polar-horizontal domain wall and compared it to a wall in which the director rotates azimuthally across the wall. The calculation involved an implicit finite-difference representation of the Euler-Lagrange equations obtained from the continuum free energy over a rectangular grid and solving them iteratively by the Newton method. The boundary conditions involved balance of elastic and anchoring torques at the substrates using the Rapini-Papoular form for the anchoring energy [9]. However, at the time we had not yet examined cells experimentally with pretilt angles sufficiently small in which polar-vertical walls would appear. For large pretilt angles at $T=T_{NI}$ our calculations [3] showed that the polar-horizontal walls are energetically more favorable, but for smaller θ_0 an azimuthal variation of the director would be more favorable energetically. However, we now find experimentally that the azimuthal variations are not observed, even for smaller values of θ_0 at $T=T_{NI}$; this suggests that we need to consider the energetics of polar-vertical domain walls. We now have performed similar calculations for the energy of

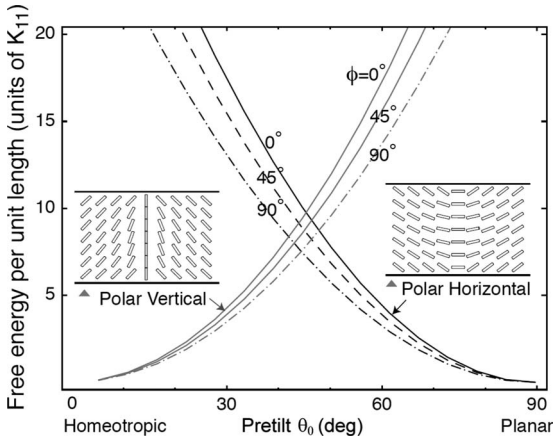

FIG. 7. Energy per unit length of domain wall vs pretilt angle θ_0 for polar-horizontal and polar vertical walls. The three sets of curves represent three different angles ($\varphi=0$, $\pi/4$, and $\pi/2$) of the director with respect to the wall, where $\Delta\varphi=\pi$ for all three cases. For this calculation the splay elastic constant $K_{11}=10^{-6}$ dyn, twist elastic constant $K_{22}=0.5\times10^{-6}$ dyn, and bend elastic constant $K_{33}=1.46\times10^{-6}$ dyn. The quadratic polar anchoring strength coefficient W_2^{θ} was taken to be 0.1 dyn cm^{-1}. The quadratic azimuthal anchoring strength coefficient W_2^{φ} was taken to be $0.1W_2^{\theta}$—i.e., 0.01 dyn cm^{-1}. Although different values of anchoring strength coefficients tend to push the energies up or down, the crossing points vary little.

polar-vertical walls (for which the director projection differs by an angle $\Delta\varphi=\pi$ across the wall) and find that such walls are less energetically favorable than polar-horizontal walls for large pretilt angles, but are more favorable when the pretilt angle is small, as expected (Fig. 7). Moreover, we also find that for reasonable values of the elastic constants and anchoring strengths [11], the polar-vertical walls are more energetically favorable than the azimuthal walls discussed in Ref. [3], as long as the azimuthal angular difference between domains is not too much smaller than π. In order to confirm and better understand these results, we applied an ac electric field to the sample. Because the liquid crystal has a negative dielectric anisotropy, this results in a larger tilt of the director in the center. It also results in a larger energy cost for all types of domain walls. We had anticipated that this energy cost could, potentially, cause the defects to move or change the anchoring conditions at the surface. Figures 8(a)–8(c) show the sample as it is cooled into the nematic, with 10 V rms at 1000 Hz applied to the cell and after the voltage has been removed. On application of a voltage we see that the cell becomes brighter, demonstrating that the tilt in the zero-voltage state is quite small. We also see that the defect structures change upon application of the voltage, but do not exhibit any discernible motion. The polar-vertical walls, in particular, undergo a Freedericksz-like transition to become azimuthal walls: The effect of the voltage is to increase the cost of the nearly vertical orientation at the center. As the director rotation through a vertical wall is close to 180°, the director at the center of the wall has a "choice;" viz., it can tilt in one of two directions at the center of the wall. Presumably, if the rotation is different from 180°, there is a bias for the director tilt so as to minimize the rotation of the order

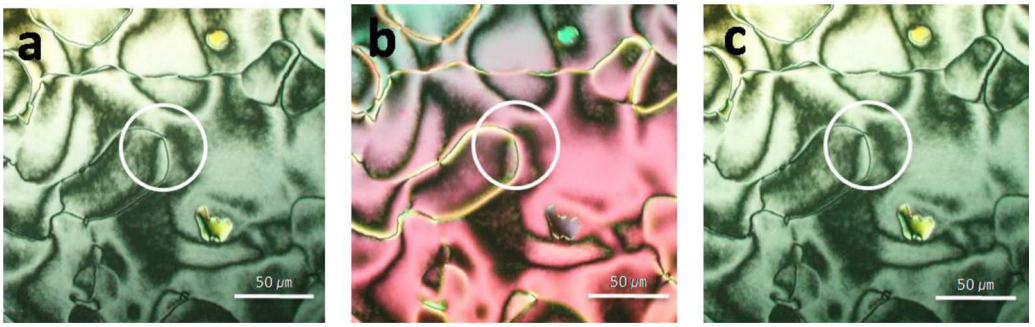

FIG. 8. (Color online) Polar-vertical domain wall passing through a point defect (see the area bounded with white circle) (a) at zero field state, (b) with 10 V at 1000 Hz applied, and (c) after voltage is removed.

parameter at the center. However, the rotation is expected to vary along the wall. In fact, we see that new point defects [white circles in Fig. 8(b)] appear in the vertical walls. Presumably, these indicate the locations where the rotation of the tilt through the (now) azimuthal walls changes sign and are point topological defects within the linear topological defects. Moreover, the width of these tilted regions through these walls is quite small, comparable to the cell thickness. This demonstrates that the surface anchoring is quite large, as the width of the wall would be inversely proportional to the surface anchoring energy coefficient divided by an elastic constant. We also note that this more highly tilted cell exhibits somewhat higher optical contrast and allows us to follow more clearly the changes in orientation of the director through the cell. This behavior confirms our identification of the nature of the defects, as we have discussed above. In addition, comparison among Figs. 8(a)–8(c) make it clear that the defects do not move. At the Freedericksz transition, the forces on the defects change substantially, such that the largest change in these forces occurs at partial disclinations. Motion of a partial disclination would decrease the length of the azimuthal wall, which, particularly since this wall has a relatively high energy subsequent to the Freedericksz transition, results in a relatively large force. However, there is no such motion. This suggests that the anchoring at the surface has become strong by the time the electric field is applied. These boundary condition issues will be the subject of subsequent investigations.

There are two important issues that need to be addressed: the simultaneous appearance of polar-vertical and polar-horizontal walls in cells treated with the same baking regimen and the apparent stability of the polar-vertical walls. Figure 7 would suggest that for a given azimuthal orientation φ with respect to the domain wall there would be a sharp crossover from polar-horizontal to polar-vertical walls at a critical pretilt angle θ_0^c. We examined the possibility that θ_0^c is a strong function of φ, so that in regions where the director projection is nearly perpendicular to the domain wall one type of wall—say, polar vertical—would nucleate and in regions where the director projection is nearly parallel the other type would nucleate. This would facilitate nucleation of both types of walls in the same cell. But for reasonable elastic constant values and over a very wide range of anchoring strengths, our calculations in Fig. 7 show that θ_0^c varies only weakly with φ. This would suggest that simultaneous nucleation of both types of domain walls would occur only for a very narrow range of pretilt angles θ_0, contrary to observations. Nevertheless, there are two mitigating conditions that may permit both types of walls to appear simultaneously over a wide range of θ_0. First, as noted in Fig. 5(a), the azimuthal angular difference $\Delta\varphi$ across the polar vertical wall may be less than π. Thus, the domain wall energy is a function not only of θ_0 and φ, but of $\Delta\varphi$ as well. Although calculation of the energy surfaces in a three-parameter space is beyond the scope of the present work, we note that the additional degree of freedom can only increase the range of θ_0 for which both types of domain walls can nucleate. But it also is important to realize that nucleation of the domain walls is not an equilibrium process. For example, one can imagine that for a given baking time t_b, the pretilt angles θ_0 may vary with position on length scales too small to observe optically, giving rise to a range of pretilt angles; it is only the spatial average $\langle\theta_0\rangle$ that we measure and report in Fig. 1. This distribution in θ_0 would necessarily allow both types of walls to occur over a wide range of baking times. Localized defects in the alignment layer also may provide nucleation sites for either type of defect wall, even when the average pretilt angle $\langle\theta_0\rangle$ would favor only one or the other type. Evidence for one or both of these mechanisms is the appearance of polar-vertical defects for pretilt angles considerably higher than predicted by the current model. Thus, it is possible that our continuum calculation provides only a rough guide to the behavior of the RTD walls—i.e., polar-horizontal walls are associated with large values of θ_0—but that the details are controlled by nucleation and kinetics, by a distribution of pretilt angles, or by a combination of both. These issues will be the subject of future work.

Turning now to the stability of the polar-vertical walls, one might assume that the wall energy could be reduced by (i) allowing the wall to widen so that the polar deviation from one domain to another takes place over a larger distance or (ii) allowing the director to "escape" to a direction perpendicular to the tilt plane of the director. Mitigating against these two possibilities is the surface anchoring, which imposes boundary conditions that prevent the director from adopting either of these two measures to reduce the overall wall energy. Certainly the existence of a nonzero W_2^θ constrains the width of the wall and prevents a reduction in $\nabla\theta$—and concomitant increase in the wall width—from one domain to the other. The escaped director mechanism, which

(if it were to exist) would be observable by a variation in the brightness of the wall as the sample is rotated between crossed polarizers, does not appear experimentally. Although this mechanism would be energetically favorable if W_2^{φ} were zero or very small, the fact that it is not observed suggests that the initially small azimuthal anchoring strength grows quickly with time in the nematic phase—this is a manifestation of the surface memory effect mentioned above [10].

To summarize, we have examined walls associated with reverse tilt domains, finding that the behavior depends critically on the initial pretilt angle as the temperature is lowered from the isotropic into the nematic phase. For sufficiently large pretilt angles θ_0 (from the vertical orientation), polar-horizontal RTD walls appear; small pretilt angles give rise to polar-vertical domain walls. These walls, which often terminate or pass through topological defects, also can exist simultaneously in the same cell, especially in cells where the pretilt angle is close to the critical pretilt θ_0^c around which there is a crossover from one type of wall that predominates to the other. Finally, although the vertical walls by themselves are, in principle, not stable, they can be stabilized by a large surface anchoring term in the free energy, which we have found develops over time by a surface memory effect.

The authors thank Dr. Ichiro Kobayashi of Nissan Chemical Industries, Ltd. for useful discussions and for providing the alignment material SE1211. This work was supported by the National Science Foundation under Grants No. DMR-0345109 and No. DMR-0804111 (C.R.) and by the Office of Naval Research under Grant No. N000140510404 (R.G.P.). J.-H.L. was supported in part by a Korean Research Foundation grant funded by the Korean government (No. KRF-2007-357-C00034). D.K. was supported by the Korean Research Foundation under Grant No. KRF-2007-013-D00070 and by Soongsil University.

[1] D. K. Shenoy, J. V. Selinger, K. A. Grüneberg, J. Naciri, and R. Shashidhar, Phys. Rev. Lett. **82**, 1716 (1999).
[2] Seo Hern Lee, Tae-Hoon Yoon, Jae Chang Kim, and Gi-Dong Lee, J. Appl. Phys. **100**, 064902 (2006).
[3] R. Wang, T. J. Atherton, M. Zhu, R. G. Petschek, and C. Rosenblatt, Phys. Rev. E **76**, 021702 (2007).
[4] G. P. Sinha, B. Wen, and C. Rosenblatt, Appl. Phys. Lett. **79**, 2543 (2001).
[5] T. Shioda, B. Wen, and C. Rosenblatt, Phys. Rev. E **67**, 041706 (2003).
[6] G. Carbone and C. Rosenblatt, Phys. Rev. Lett. **94**, 057802 (2005).
[7] A. J. Pidduck, G. P. Bryan-Brown, S. D. Haslam, and R. Bannister, Liq. Cryst. **21**, 759 (1966).
[8] Z. Huang and C. Rosenblatt, Appl. Phys. Lett. **86**, 011908 (2005).
[9] A. Rapini and M. Papoular, J. Phys. (Paris), Colloq. **30**, C4–54 (1969).
[10] N. A. Clark, Phys. Rev. Lett. **55**, 292 (1985).
[11] L. M. Blinov, A. Yu. Kabayenkov, and A. A. Sonin, Liq. Cryst. **5**, 645 (1989).